Imaging Neuroscience
an open access journal

Research Article

The effect of cerebellar TMS on error processing: A combined single-pulse TMS and ERP study

Adam M. Berlijn[a,b,c,*], Dana M. Huvermann[a,d,*], Stefan J. Groiss[c,e], Alfons Schnitzler[c,e], Manfred Mittelstaedt[a], Christian Bellebaum[a], Dagmar Timmann[d], Martina Minnerop[b,c,e], Jutta Peterburs[a,f]

[a]Faculty of Mathematics and Natural Sciences, Heinrich Heine University Düsseldorf, Düsseldorf, Germany

[b]Institute of Neuroscience and Medicine (INM-1), Research Centre Jülich, Jülich, Germany

[c]Department of Neurology, Center for Movement Disorders and Neuromodulation, Medical Faculty, Heinrich-Heine University Düsseldorf, Düsseldorf, Germany

[d]Department of Neurology and Center for Translational and Behavioral Neurosciences (C-TNBS), Essen University Hospital, University of Duisburg-Essen, Essen, Germany

[e]Institute of Clinical Neuroscience and Medical Psychology, Medical Faculty & University Hospital Düsseldorf, Heinrich Heine University Düsseldorf, Düsseldorf, Germany

[f]Institute for Systems Medicine & Department of Human Medicine, MSH Medical School Hamburg, Hamburg, Germany

*Shared first authorship

Corresponding Author: Adam M. Berlijn (berlijn@uni-duesseldorf.de)

ABSTRACT

The present study investigated temporal aspects of cerebellar contributions to the processing of performance errors as indexed by the error-related negativity (ERN) in the response-locked event-related potential (ERP). We co-registered EEG and applied single-pulse transcranial magnetic stimulation (spTMS) to the left posterolateral cerebellum and an extra-cerebellar control region (vertex) while healthy adult volunteers performed a Go/Nogo Flanker Task. In Go trials, TMS pulses were applied at four different time points, with temporal shifts of -100 ms, -50 ms, 0 ms, or +50 ms relative to the individual error latency (IEL, i.e., individual ERN peak latency + median error response time). These stimulation timings were aggregated into early (-100 ms, -50 ms) and late (0 ms, +50 ms) stimulation for the analysis. In Nogo trials, TMS pulses occurred 0 ms, 100 ms, or 300 ms after stimulus onset. Mixed linear model analyses revealed that cerebellar stimulation did not affect error rates overall. No effects were found for response times. As hypothesized, ERN amplitudes were decreased for cerebellar stimulation. No significant differences were found for the error positivity (Pe). Similar to TMS application to probe cerebellar-brain inhibition in the motor domain, the inhibitory tone of the cerebellar cortex may have been disrupted by the pulses. Reduced inhibitory output of the cerebellar cortex may have facilitated the processing of error information for response selection, which is reflected in a decreased ERN.

Keywords: Error processing, cerebellum, cognitive control, EEG, single pulse TMS, performance monitoring, executive functions

1. INTRODUCTION

The cerebellum is assumed to be strongly involved in making predictions, processing error information, and adjusting behavior not only in the motor but also in the cognitive domain (King et al., 2019; Sokolov et al., 2017). Specifically, it has been suggested to generate internal models of movement and thought that are crucial for efficiency and precision in adaptive control (Ito, 2008; Koziol et al., 2014; Wolpert et al., 1998). These internal models reflect the process of error detection and correction in

Received: 3 August 2023 Revision: 24 November 2023 Accepted: 29 December 2023 Available Online: 16 January 2024

which the cerebellum functions as a comparator, comparing the actual and predicted outcomes of actions and adjusting the predictions accordingly. Along these lines, performance monitoring, which includes error and feedback processing, has been proposed to be an overarching function of the cerebellum (Peterburs & Desmond, 2016).

Performance monitoring can be indexed by the error-related negativity (ERN) in the event-related potential (ERP) in the electroencephalogram (EEG). The ERN, a relative negativity that typically peaks within 100 ms after an erroneous response, is interpreted to reflect processes related to the detection of errors (Falkenstein et al., 1991; Gehring et al., 1993) or response conflict (Botvinick et al., 2001; Yeung et al., 2004). The ERN has a symmetric, frontocentral scalp distribution, and its neural generator is likely in the anterior cingulate cortex (ACC) or supplementary motor area (Dehaene et al., 1994; Herrmann et al., 2004). It has been proposed that the ACC is critical for detecting conflict and conveying conflict-related information to other brain regions such as the lateral prefrontal cortex (Cohen et al., 2000). The ACC is also a key structure for evaluating actions and their outcomes, thus playing a critical role for reinforcement learning (Holroyd & Yeung, 2011).

Findings from studies in patients with cerebellar diseases suggest that the cerebellum contributes to the processing of errors and response conflict. Specifically, the ERN was shown to be reduced in patients with focal post-acute vascular lesions of the cerebellum (Peterburs et al., 2012) and cerebellar degenerative disease (Peterburs et al., 2015). The latter patient group also exhibited increased error rates, and the ERN reduction and behavioral impairment were linked to gray matter volume loss in posterolateral cerebellar regions (Peterburs et al., 2015). In contrast, patients with post-acute cerebellar lesions did not show altered behavior. However, another ERP component related to error processing, the error positivity (Pe), a relative positivity occurring 200–400 ms post-response that has been linked to more conscious aspects of error processing (Falkenstein et al., 1995), was increased (Peterburs et al., 2012). Interestingly, the Pe was unaffected in patients with progressive cerebellar degeneration (Peterburs et al., 2015). This result pattern could be indicative of a compensatory mechanism that may help maintain behavioral performance in patients with longstanding lesions but is absent in patients with cerebellar degenerative disease. In contrast, Tunc et al. (2019) investigated error processing in patients with different types of spinocerebellar ataxia (SCA) and failed to find behavioral impairments beyond a slowing of response times. However, they did report a trend-level reduction of the ERN in patients compared with healthy controls, which conforms to previous findings (Peterburs et al., 2015). The less pronounced neurophysiological differences and discrepancy in behavioral results compared with the study by Peterburs et al. (2015) may be attributed to sample differences (e.g., SCA subtypes with extra-cerebellar degeneration included in the study by Tunc et al., differences in extent and location of cerebellar degeneration). Cerebellar degeneration in Crus I, Crus II, and the deep cerebellar nuclei may cause stronger effects on error processing than the degeneration of other, more motor control related regions of the cerebellum, such as the anterior regions (see King et al., 2019 for a detailed overview on different cognitive functions reflected in different regions of the cerebellum).

While these patient studies provided strong evidence for a role of the cerebellum in error processing, testing patients is not the only option to probe such cerebellar involvement. An alternative approach that offers the possibility of direct manipulations of brain activity is to use non-invasive stimulation of the cerebellum. Transcranial magnetic stimulation (TMS) is a widely used non-invasive brain stimulation technique that can be applied to a variety of brain regions (for a review, see Grimaldi et al., 2014) to establish causal links to behavior (see Vaidya et al., 2019). Single-pulse TMS (spTMS) is assumed to be useful for both facilitation (Shirota et al., 2012) and disruption of neuronal processes (Pascual-Leone, 1999) and can be used in fast-paced task designs (Verleger et al., 2009). A number of studies have targeted the cerebellum with TMS, among other techniques, to investigate cerebellar-brain inhibition (Ugawa et al., 1995; Fernandez et al., 2018). For instance, Ugawa et al. (1995) demonstrated that the motor cortex could be influenced by stimulating the cerebellum. The cerebellar cortex inhibits the deep cerebellar nuclei, which are the only output source of cerebellar projections to higher cortical regions via the thalamus (Palesi et al., 2017). The TMS pulse triggers activity of the cerebellar cortex that suppresses motor cortical excitability in M1 via increased inhibition of the cerebellar nuclei. Notably, effects of cerebellar TMS have also been reported in the non-motor domain. Stimulation of the right superior cerebellum led to increased response times in a verbal working memory task (Desmond et al., 2005) and disrupted phonological prediction (Sheu et al., 2019). We, thus, assume the influence of spTMS on the cerebellum to be similarly disruptive for other cognitive domains like the processing of performance errors.

Mannarelli et al. (2020) used cathodal transcranial direct current stimulation (tDCS) to the cerebellum before healthy participants performed a Go/Nogo task. In contrast to the facilitating effects of anodal tDCS, cathodal tDCS causes a hyperpolarization of neurons, making upcoming action potentials harder to trigger. After cerebellar tDCS compared with sham stimulation, the Nogo-N2, a negative ERP component peaking around 250–300 ms post stimulus onset (Folstein & van Petten, 2008), was reduced. The N2 has been linked to response inhibition and cognitive control, with decreased amplitudes indicating improved performance monitoring in terms of cognitive flexibility (Larson & Clayson, 2011). In addition, false alarm rates were increased. These results provide the first evidence that cerebellar neuromodulation alters behavioral and ERP indices of performance monitoring and cognitive control. In particular, it has been suggested that the stimulus-locked N2 and the response-locked ERN may reflect activity of the same underlying error monitoring system (Ferdinand et al., 2008; Folstein & van Petten, 2008; van Veen & Carter, 2002). Hence, perturbing cerebellar function by non-invasive brain stimulation should also affect error processing and the ERN, and this is what the present study aimed to demonstrate. However, it must be noted that findings on effects of cerebellar tDCS on cognition and motor behavior have been rather heterogeneous and inconsistent (Jalali et al., 2017), and the exact mechanisms on the cell or network level are still unclear (van Dun et al., 2017). TMS, on the other hand, allows for a more focal and controlled stimulation that can reach deeper regions in the brain by generating pulses in a time resolution of less than 1 ms (Koponen et al., 2018). Therefore, the present study made use of cerebellar spTMS (and stimulation of vertex as a control site) in a Go/Nogo Flanker Task (Voegler et al., 2018) to investigate effects on error processing. Guided by the previous patient studies (Peterburs et al., 2012, 2015), our main focus was on the response-locked ERP components ERN and Pe. The stimulus-locked ERP components Nogo-N2 and Nogo-P3 investigated in the previous tDCS study in healthy subjects (Mannarelli et al., 2020) were not the focus of the present work, so data on and analyses of these components are only provided as Supplementary Material. For a more comprehensive neurophysiological account, we have also exploratively analyzed induced theta power in the time-frequency domain as an index of cognitive control (e.g., Cavanagh & Frank, 2014). Information on preprocessing, results, and discussion with respect to these dependent variables is provided in the Supplementary Material (see Figs. S11–S14).

We selected the left lateral cerebellum for stimulation with a double cone TMS coil because of several studies pointing towards the significance of posterolateral cerebellar regions for executive functions, which also encompass error processing (King et al., 2019; Sheu et al., 2019; Stoodley & Schmahmann, 2009). The experiment was conducted on two different days resulting in a fully within-subject design (each participant underwent both cerebellum and vertex stimulation). We followed the study design by Verleger et al. (2009) in which an spTMS pulse was delivered in each trial of a Flanker Task. As outlined above, spTMS has a high temporal resolution, and it can thus help elucidate causal links between brain and behavior. Thus, spTMS can also help elucidate temporal aspects of cerebellar contributions to error processing. Verleger et al. (2009) temporally shifted the pulses depending on an individually estimated peak latency of the lateralized readiness potential, a potential reflecting motor cortex activity leading up to voluntary movements, which was measured before the TMS blocks. In the present study, pulses were delivered at four different time points relative to the individual error latency (IEL, i.e., individual ERN peak latency + median error response time) in Go trials, and at three different time points relative to stimulus onset in Nogo trials.

Similar to deficits found in patients with cerebellar degeneration (Peterburs et al., 2015), we expected increased error rates in Go trials for cerebellar TMS compared to vertex TMS, but only when pulses were delivered before the responses, due to disturbance of the internal forward-model generated within the cerebellum (see Ramnani, 2006). Concerning the ERN, patients with cerebellar damage showed reduced negativity in the error-correct difference signal in the typical ERN time window (Peterburs et al., 2012, 2015). Consequently, we expected a reduced ERN for cerebellar TMS compared to vertex for pulses that were applied 100 ms and 50 ms before the IEL, since these time points should precede the onset of error processing. Since the Pe in patients with cerebellar lesions was interpreted to be the result of long-term compensatory processes of the brain (Peterburs et al., 2012), we did not expect effects of cerebellar spTMS on the Pe. Further, more exploratory hypotheses regarding response inhibition in Nogo trials as reflected in Nogo-N2 and Nogo-P3 and an additional analysis on the induced theta power are provided and discussed in the Supplementary Material.

2. METHODS

2.1. Sample

Twenty-five young and healthy participants were recruited through newspaper advertisements and postings at Heinrich-Heine-University Düsseldorf. Data from nine participants had to be excluded from the analyses: two participants attended only the first appointments necessary for study completion, further two participants complained of mild headaches during the task and dropped out, a miscalculated TMS onset value was used in another two participants, two participants made too few errors in the main task, and another misunderstood the task. Concerning the pre-task, which was used to determine the individual error latency (IEL, see below), we aimed to repeat the Go/Nogo Flanker until participants who committed at least six errors in all conditions, because at least six error trials are needed to reliably measure the ERN (see Olvet & Hajcak, 2009; Pontifex et al., 2010). For one participant we only discovered post hoc, after trial inspection and removing double responses, that only five error trials in one condition remained (see Table S1 in the Supplementary Material). As the ERN was clearly visible after averaging the five error trials, we decided to include the participant in further data analysis. The final sample thus consisted of 16 participants. The required sample size was estimated based on studies which used cerebellar spTMS in a different task (n = 17, Desmond et al., 2005; n = 10, Panouillères et al., 2012; n = 23, Sheu et al., 2019), or spTMS at another location in a Flanker task (n = 20, Danielmeier et al., 2009; n = 21, Klein et al., 2014; n = 8, Soto et al., 2009; n = 12, Verleger et al., 2009). Participants were healthy adults (age range 19–32 years, M = 24.00 years, SD = 3.70, n = 13 females, n = 12 right-handed and n = 1 ambidextrous; for more details, see Table S1 in the Supplementary Material). As TMS uses electromagnetic pulses, exclusion criteria were metal parts within the body (e.g., implants, pacemakers, shards of metal, pumps for medication), spinal fractures, acute heart attacks, or pregnancy. Further exclusion criteria were current psychiatric disorders, neurological disorders, alcohol or substance abuse, and intake of medication affecting the central nervous system. Participants were paid 40 Euros for participating in the two appointments. All participants gave written informed consent. The study was preregistered on the Open Science Framework (OSF: https://osf.io/6v9pa) and was approved by the Ethics Committee at the Faculty of Medicine of Heinrich Heine University Düsseldorf in accordance with the Declaration of Helsinki.

2.2. Questionnaires

Participants had to fill in a demographic questionnaire as well as the "Mehrfachwahl-Wortschatz-Intelligenztest" (IQ: M = 98.75, SD = 10.88; Lehrl et al., 1977), a multiple-choice vocabulary intelligence test.

2.3. Go/Nogo Flanker task

Participants completed a modified Go/Nogo Flanker task coded in the software *Presentation* (version 20.0, Build 02.20.17, Neurobehavioral Systems, Inc.). Figure 1 provides a schematic illustration of the time course and sequence of stimulus presentation in each trial. The main task consisted of 600 trials in four blocks. Go trials made up 80 % of all trials (480 trials), while Nogo trials made up 20 % of all trials (120 trials). In 80 % of Go Trials (384 trials), the flanker arrows aligned with the central target arrow (congruent trials), while in the other 20 % of Go trials (96 trials), the flankers pointed in the opposite direction (incongruent). Each trial started with the onset of arrow flankers positioned above and below a fixation cross for 200 ms. During Go trials, the fixation cross was replaced by the central target arrow to which participants had to respond by pressing the corresponding (left or right) button on a response pad with the index or middle finger of their right hand, respectively. Participants were instructed to respond as fast and as accurately as possible. If participants did not press one of the two buttons within the response time window of 350 ms (alternatively 400 ms, when the miss rate was too high in the flanker pre-task), a reminder to respond faster was displayed. No feedback was provided concerning the correctness of the response. During Nogo trials, the fixation cross was replaced by a filled circle, to which participants should suppress their response and not press a button. As in Go trials, the flankers together with the circle were displayed in the response time window for 350/400 ms. Thereafter, a fixation cross without flankers was displayed for 500 ms. During the subsequent inter-trial interval, the fixation cross was presented for a further 900–1300 ms (jittered).

Since the aim of the present study was to disturb error processing on a trial-by-trial basis using TMS pulses applied to the cerebellum and to elucidate temporal aspects of cerebellar involvement in error processing, it was critical to determine the time point at which cerebellar input was needed for error processing. More specifically, cerebellar input could be needed at the very onset of error processing or a bit later when error processing is already underway. To temporally approximate the onset of error processing individually for each participant, we

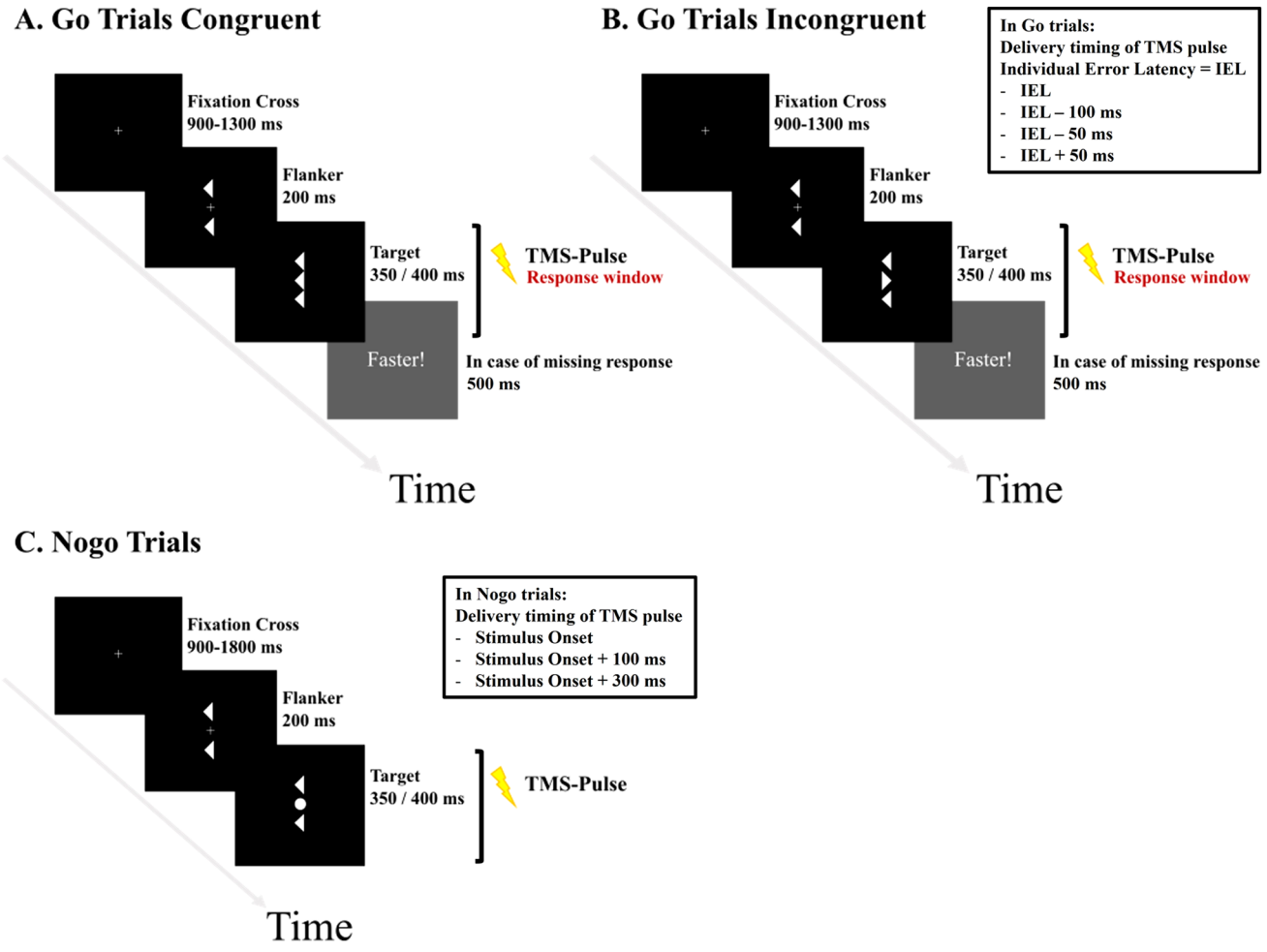

Fig. 1. Schematic illustration of time course and sequence of stimulus presentation in a trial of the Go/Nogo Flanker Task. Go trials with congruent flankers (A) and with incongruent flankers (B) relative to the target arrow in the center. Only one single pulse was applied in each trial. TMS pulses were delivered for Go trials shortly before the IEL (-100 ms, -50 ms), at the IEL, or shortly after the IEL (+50 ms). (C) In Nogo Trials, the target stimulus indicating the need to inhibit the response was a circle. TMS pulses were delivered at stimulus onset or shortly after target onset (+100 ms or +300 ms).

determined the IEL using a Flanker pre-task without pulses. This Flanker pre-task consisted of the same ratio of Go and Nogo Trials as the main task (120 trials in total, 80 Go and 40 Nogo trials). The IEL was calculated by adding the median error response time to the latency of the ERN in the response-locked ERP. If a participant was unable to respond within the standard response time window of 350 ms in more than 25 % of trials in the pre-task, the task was repeated with an increased response time window of 400 ms. This was done to ensure that enough valid trials were recorded. In total, three participants required the longer response time window.

Throughout the Flanker main task, monophasic single TMS pulses were applied within each trial. The time points at which TMS was applied differed for Go and Nogo trials. In Go trials, TMS pulses were delivered at the IEL (0 ms) as well as 100 ms before (-100 ms), 50 ms before (-50 ms), and 50 ms after (+50 ms). In Nogo trials, TMS pulses were delivered at fixed time points, that is, at stimulus onset as well as 100 ms and 300 ms after stimulus onset (+100 ms and +300 ms, respectively). Pulse timings relative to the IEL in Go and relative to stimulus onset in Nogo trials were randomized throughout the task but occurred an equal number of times per trial type and block.

2.4. Procedure

Upon arriving at the laboratory, the participants were seated in a brightly lit room in front of a laptop (DELL®

Precision M4800, 15.4 inch with a resolution of 1920 × 1080 pixels and a refresh rate of 60 Hz) with a response box (Cedrus RB-740, Science Plus Group, Groningen, NL) positioned before it. The distance between response box and laptop was kept constant. Only two keys were relevant for the task and had to be pressed with the index (left key) and middle finger (right key) of the right hand. A third key was used to navigate through pauses and instruction slides. After positioning the participants and putting earplugs in their ears, the EEG cap was aligned on the head, and the scalp electrodes were prepared. The electrodes on the cap were further covered with a plastic wrap to avoid any direct contact between electrodes and the TMS coil which could cause artifacts (Hernandez-Pavon et al., 2023). EMG electrodes were attached to the left hand, and the TMS stimulators were started and triggered via the laptop so that pulses were sent for the determination of the individual motor threshold (IMT). After IMT determination, the coil was firmly aligned and fixed with a custom mounting structure. Thereafter, the Flanker pre-task was started, in which no pulses occurred. Subsequently, another experimental task with spTMS was completed, which is not part of this manuscript. While participants were completing this task, we calculated the individual ERN peak latency and median response time for errors as described above. Subsequently, the IEL was calculated and used as an input value for the Flanker main task. Afterwards, the Flanker main task was performed. Participants underwent cerebellar and vertex stimulation in separate appointments. They were aware that both sessions included stimulation, but they were not explicitly informed about the specifics of the two stimulation sites. They were also naïve to the study's intent. The two appointments took place with a temporal gap of at least 48 hours (M = 82.13 days, SD = 143.36 days, range from 2 to 373 days). Due to a defect in the TMS stimulators, the second measurement had to be postponed for a long time, resulting in time gaps of 362 to 373 days for 3 subjects. Correcting for the delay of these subjects, the time interval between the two appointments was on average only 16.00 days (SD = 20.52 days, range from 2 to 74 days). The order of the stimulation sites was counterbalanced.

2.5. TMS-EEG-EMG interface

2.5.1. EEG system

A TMS compatible amplifier (BrainAmp MR plus, BrainProducts GmbH, Munich, Germany) was used with a cap containing 32 flat multitrodes. The flat electrodes minimize the distance between the coil and the skull surface. The following electrode sites were used: Fp1, Fp2, Fz, F3, F4, F7, F8, FCz, FC1, FC2, FC5, FC6, Cz, C3, C4, CPz, CP1, CP2, CP5, CP6, T7, T8, Pz, P3, P4, P7, P8, Oz, O1, and O2. BrainVision Recorder software, version 1.21 (BrainProducts, Munich, Germany) was used for recording. Impedances were kept below 5 kΩ. Data were sampled at 1000 Hz.

2.5.2. EMG system

Two surface EMG Ag/AgCl-electrodes (20 × 15 mm, Ambu, Ballerup, Denmark) were placed on the left M. abductor pollicis brevis in resting condition to record the muscle activity in terms of motor evoked potentials (MEPs) that reflect the corticospinal excitability throughout the estimation period of the IMT. This also allowed us to check that no MEPs would be triggered by the TMS pulses during the tasks. The signal was amplified with a Digitimer D360 (Digitimer Ltd, Hertfordshire, UK). The frequency band of the filter was 100–5000 Hz and digitized at a sampling rate of 5 kHz (Signal version 6.02, Cambridge Electronic Design Ltd., Cambridge, UK).

2.5.3. TMS system

We estimated the IMT with a custom script in *Presentation* that sent a code to a single TMS stimulator (Magstim® 200²) every 10 seconds to elicit a pulse. The double cone coil was aligned so that we could stimulate the right motor cortex (region M1). After an MEP was detected in the EMG signal using the independent trigger mode in the software *Signal*, 5 consecutive trials (out of 10) were counted to determine whether the position also clearly stimulated the motor cortex. The output power of the device was then reduced until only 5 out of 10 trials elicited an MEP. The estimated IMT with additional 20 % power (corresponding to 120 % motor threshold) was used as the output power for the TMS system for both appointments. Nevertheless, we measured the motor-threshold on both appointments to see if there was any variability. Checking the IMT revealed no significant difference between the first (M = 38.20 %, SD = 7.84 %) and second appointment (M = 37.68 %, SD = 7.97 %), $t(37)$ = 0.20, p = .840, and no significant difference between the cerebellar (M = 37.80 %, SD = 8.15 %) and vertex (M = 38.11 %, SD = 7.64 %) stimulation appointments $t(37)$ = -0.12, p = .905. The TMS coil was either placed at the level of the left lateral cerebellum (3 cm left and 1 cm inferior to the inion; Hardwick et al., 2014) or at

the vertex position which corresponds to electrode position Cz of the international 10–20 system (Pizem et al., 2022, see Fig. 2 for an illustration, and Figs. S15 and S16 for real photographs in the Supplementary Material) with the voltage flow in the inferior direction. After the coil was correctly aligned, it was fixed with a custom stand so that the same position was maintained over the course of the session. In addition, we used a fabric elastic band to ensure that the coil-to-head distance was kept constant (forehead for the cerebellar TMS or chin for the vertex TMS). The distance of the coil to the head surface was observed during the task and adjusted during the pause between the individual, since even small changes lead to a decrease in the induced magnetic field strength (Hernandez-Pavon et al., 2023).

The BiStim TMS stimulators were manually charged before the first trial, and the independent trigger mode was selected in Signal for the subsequent tasks to trigger the stimulators. Then, the single-pulses were observed in the EMG-signal to ensure that no MEPs were evoked, particularly when stimulating the cerebellum. If MEPs had occurred, the session would have been interrupted, and the coil would be realigned, in order to avoid co-stimulating the brainstem. However, this did not occur during our study. Additionally, the coil position was constantly monitored and readjusted between the blocks and tasks if substantial movement had occurred to ensure that the distance between coil and scalp was consistent. Since the recharge period of a single Magstim® 200² stimulator exceeded the duration of a single trial, we alternated activation of two BiStim stimulators. Unfortunately, due to overheating of the stimulators, trials were lost in 3 participants towards the end of the task, for the TMS system no longer sent any pulses while the task and EEG measurements were still running. The time of termination was checked in the EEG signal, so that all trials without TMS pulses were excluded from analysis. The heat development in the stimulators was related to both

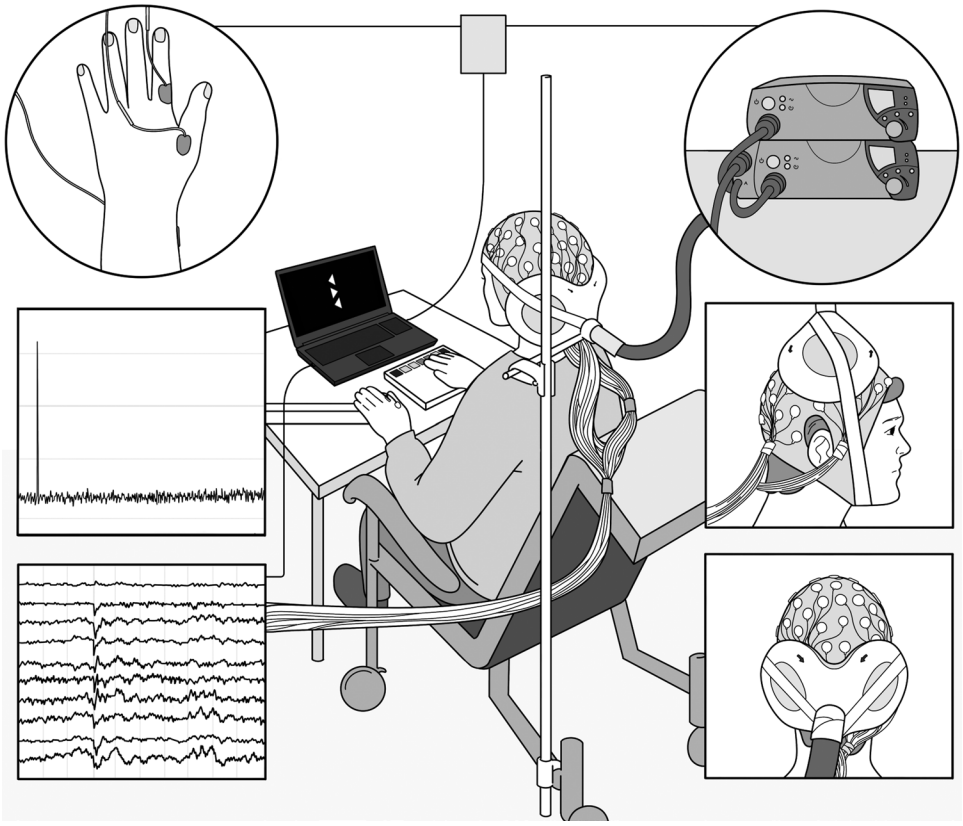

Fig. 2. Illustration of the TMS-EEG Setup for cerebellar and vertex stimulation. Top left circle shows the placement of the electrodes for recording of the EMG signal. Below, the TMS pulse is shown in the EMG signal. Bottom left, continuous measures of the EEG signal. Top right, TMS generators are shown. Below, the TMS coil orientation for vertex stimulation is shown and, in the bottom, right, the coil alignment for the cerebellar stimulation is presented. The voltage flow indicated by the arrows is aligned inferiorly. A double-cone coil was used for stimulation.

the high number of single pulses and the output power which varied greatly among the participants (see Table S1 in the Supplementary Material).

In case of a port conflict due to close proximity of two marker codes sent by the presentation laptop to the EEG system (i.e., codes sent within 5 ms), which may be the case for the response codes and matching TMS pulse codes, the later code was delayed until the port conflict no longer arose. The respective code timings were corrected in the EEG marker file using a custom script in MATLAB. Time points were not changed for the TMS pulse codes because the timing in the marker file always fitted the timing of the real TMS pulse. Instead, trials with a TMS pulse differently timed than the planned onset due to marker code delay were excluded.

2.6. Individual error latency estimation based on the flanker pre-task

ERN latency was determined by peak detection performed in BrainVision Analyzer software, version 2.1 (BrainProducts, Munich, Germany). All trials containing two or more responses were removed beforehand. Preprocessing for peak detection was performed as follows: First, data were re-referenced to the average signal of all electrodes, and the signal at FCz was re-established. Next, a DC detrend was performed, followed by low-pass filtering with a cut-off of 30 Hz and a slope of 12 dB/oct, high-pass filtering with a cut-off of 0.1 Hz and a slope of 12 dB/oct, and a notch filter set to 50 Hz. Subsequently, automatic ocular correction ICA was performed, and data were segmented into epochs of 600 ms, starting 200 ms before and ending 400 ms after erroneous responses. The baseline-corrected data (with the 200 ms period preceding response onset as baseline) underwent artifact rejection (only 3 trials were rejected across all participants and sessions) with the following settings: maximum difference of values over 100 µV or activity lower than 0.1 µV within an interval of 100 ms, voltage steps exceeding 50 µV/ms, or values above 100 µV or below -100 µV. Segments were then averaged, and peak detection was performed on a time window of 100 ms after the response, searching for a negative peak at site FCz.

2.7. Dependent variables

Behavioral outcome variables were error rates and response times in Go trials. For the EEG data, we analyzed the ERN for Go Trials in the response-locked ERP. In an exploratory analysis, the Pe (Go trials) was also analyzed. The ERN was defined as the local maximal negative peak in the error-correct difference signal within a time window of 100 ms post-response at site FCz (see Hajcak & Foti, 2008). The Pe was defined as the maximum positive peak in the difference signal within the time window between 200 and 400 ms post-response at Pz (see Larson et al., 2010). Follow-up analyses with the original waveforms were conducted to further elucidate if effects were specifically driven by altered ERP amplitudes for errors or correct responses. In addition, analyses of false alarm rates and Nogo-N2 and Nogo-P3 ERP components as well as analyses of induced theta power in the time-frequency domain are provided in the Supplementary Material.

2.8. Preprocessing of the TMS-EEG data

Preprocessing of the spTMS-EEG co-registered EEG raw data was conducted using the EEGLAB Toolbox (version 2021.1) in MATLAB (version R2021a) (MathWorks, Natick, Massachusetts, USA) and the Automated aRTIfact rejection for Single-pulse TMS-EEG Data (ARTIST) algorithm created by Wu et al. (2018). This algorithm provides an efficient and objective approach to preprocess raw EEG data and has proven to be superior to manual artifact rejection by experts and other algorithms such as TESA (Rogasch et al., 2017; Wu et al., 2018). Some of the default settings were adapted because the signal at electrode FCz, which had been used as online reference during EEG recording, needed to be re-established. In addition, the high pass filter of 1 Hz was kept, and the low pass filter was changed from 100 Hz to 30 Hz. The notch filter was changed from 60 Hz to 50 Hz. Electrode Iz was removed before applying the ARTIST algorithm because of low signal quality. The ARTIST algorithm creates segments around a given code which marks the onset of the TMS pulse. Here, segments were created with a length of 2500 ms, spanning 1000 ms before and 1500 ms after TMS pulse onset. Next, response onsets were checked by a custom script using MATLAB to ensure that only valid trials were included into the analysis (see above, some responses and therefore the respective response codes had overlapped with other codes within trials and were therefore delayed). In addition, we manually rejected trials without a TMS pulse (due to overheating or close proximity of two TMS pulses, see above) before re-referencing and segmenting the data. Following this, the ARTIST algorithm preprocessed the data in three distinct stages. In the first stage, large-amplitude artifacts were removed by applying DC drift correction, the removal and

interpolation of the TMS pulse artifact (15 ms prior to the TMS marker code onset until 5 ms after), downsampling of the data, and the removal of the TMS decay artifacts in a first ICA run. In the second stage, the AC line noise was removed, and the band-pass filter was applied. Then, the signal was segmented around the TMS pulse onset, and segments that exceeded the default thresholds were removed. The final step within the second stage was the removal and interpolation of poor channels. ARTIST interpolated on average 1.13 channels (*SD* = 1.13) per participant and stimulation site. In addition, on average, 44.13 trials (*SD* = 50.93) were rejected, including both trials which were manually rejected due to overheating (*M* = 29.25, *SD* = 39.67, range = 5–169) and trials which ARTIST rejected (*M* = 14.88, *SD* = 14.72, range = 1–63), with slightly more excluded trials in total for cerebellar (*M* = 47.56, *SD* = 54.69) compared to vertex (*M* = 40.69, *SD* = 48.41) stimulation (*N* = 16). In the third stage, poor independent components were removed in a second ICA run. The data average was referenced, and the baseline was corrected. The output data were imported into BrainVision Analyzer 2.1, and further segmentation was performed according to trial type (Go/Nogo). For Go trials, segmentation was done for response and stimulus onset separately for error and correct trials. The adapted scripts and raw data can be found in the following OSF folder: https://osf.io/jwfn9/

2.9. Statistical models

We deviated from our preregistration and ran mixed linear model (MLMs) analyses in R (R Core Team, version 4.0.3) using RStudio Team (2020: version 1.3.959) and the lme4 package (version: 1.1.25, Bates et al., 2014) in place of traditional repeated-measures ANOVA. This enabled us to analyze factors with missing values and use the participant as a random factor to further explain variance in the data. Meteyard and Davies (2020) proposed in their best practice guidelines for MLMs that the maximum model should be chosen, including all within-subject main and interaction effects as random effects. The maximum model should be only chosen if no errors in the model fit, in terms of converging errors or singular fits, appear, which would cause an overfitting of the model. To avoid this, the models were checked using an iterative process in which the within-subject highest order interaction was first included as random factor and the random slopes rejected subsequently in case of model fit errors. All our models included stimulation site and stimulation timing as fixed effects, but for some models, these factors were additionally included as random slopes depending on the model fit. In addition, Cooks distance (Cook, 1977) was calculated to identify potential outlier subjects before running the MLM analysis using the influence.ME package (version 0.9–9; Nieuwenhuis et al., 2012).

Before setting up our models for ERP analysis in Go trials, we grouped the four stimulation timings into a two-level factor, resulting in "early" and "late" stimulation. For this purpose, the -100 ms and -50 ms trials were combined into "early" and the 0 ms (at IEL) and +50 ms trials into "late." This allowed us to pool more error trials together, to better take into account the variability of the IEL within and across participants, and to compare the effect of stimulation timing on error processing over a broader time period.

To check for baseline performance differences between the two sessions in the Flanker pre-task, we calculated Linear models (LMs) comparing error rates (Go trials) and ERN amplitude between the cerebellar stimulation and vertex stimulation session (see Fig. S1 and Table S3 in the Supplementary Material).

To analyze behavioral performance in the Flanker main task for Go trials, we set up an MLMs for error rates including stimulation site (cerebellum, vertex), stimulation timing (early, late), and the interaction between these factors as fixed effects and added stimulation site and the interaction with stimulation site and stimulation timing as random slopes and participant as random effect in the model.

$$\text{Error rate} \sim \text{site} * \text{timing} + (1 + \text{site} + \text{site} : \text{timing} \mid \text{participant})$$

For response times, we included all responses to see whether there was a difference in response times between correct and error trials. In the final model, we included trial type (correct trials, error trials) as fixed effect and as random slope into the model equation.

$$\text{Response time} \sim \text{site} * \text{timing} * \text{trial type} + (1 + \text{site} * \text{trial type} \mid \text{participant})$$

In a third MLM, we analyzed error responses by their timing relative to TMS onset to identify a possible influence of the pulse itself on the error rates independent of the trial type. Here, the model was specified using the error rates as the dependent variable, stimulation site (cerebellum, vertex) and TMS timing (response preTMS, response postTMS) as fixed effects and random slopes:

$$\text{Error rate} \sim \text{site} * \text{TMStiming} + (1 + \text{site} + \text{site} : \text{TMS timing} \mid \text{participant})$$

For ERP analyses for Go trials, we analyzed the ERN and Pe peak amplitudes obtained from the difference wave as the dependent variables.

$$\text{ERN\_diff}(\text{amp}) \sim \text{site} * \text{timing} + (1 + \text{site} + \text{timing} \mid \text{participant})$$

$$\text{Pe\_diff}(\text{amp}) \sim \text{site} * \text{timing} + (1 + \text{site} \mid \text{participant})$$

In addition, we analyzed the original waveforms, entering the amplitudes at the time points corresponding to the ERN latency in the difference signal. We added fixed effects of stimulation site (cerebellum, vertex) and timing (early, late) and trial type (correct trials, error trials) for the analysis as well as the interaction between the fixed effects as well as the three factors as random slopes and participant as a random effect. In addition, the optimizer was changed from the default to Nelder-mead to cope with an occurring convergence error as suggested by the best practice guideline by Meteyard and Davies (2020).

The final, maximum model specification was as follows:

$$\text{ERN}(\text{amp}) \sim \text{site} * \text{timing} * \text{trial type} + (1 + \text{site} + \text{timing} + \text{trial type} + \text{site} : \text{timing} \mid \text{participant})$$

We simple-coded the categorical predictors stimulation site (0.5 = cerebellum, –0.5 = vertex), stimulation timing (0.5 = early, –0.5 = late), and trial type (0.5 = correct, –0.5 = error). Also, TMS-timing (response pre-TMS = 0.5, response post-TMS = –0.5) was simple-coded for the additional analysis of the error rate. We used the lmerTest package (version: 3.1.3, Kuznetsova et al., 2017) in R using Satterthwaite's method to estimate the degrees of freedom and to generate *p*-values for MLMs. We considered *p*-values below .05 as statistically significant. Statistical models for the analyses of false alarms, Nogo-N2, and Nogo-P3 are provided in the Supplementary Material.

3. RESULTS

3.1. Error rates

MLM analysis revealed no significant effects of stimulation site or timing on error rates (all $p \geq .384$, $n = 15$, see Fig. 3A). However, exploring the influence of TMS timing relative to response execution (i.e., whether a pulse had occurred prior to a response on a given trial or after the response) revealed a highly significant main effect of TMS timing ($\beta = 5.02$, $t(15.00) = 13.30$, $p < .001$, see Fig. 3B). Error rates were higher in trials in which pulses had occurred after the response (i.e., response pre-TMS: $M = 13.69$ %, $SD = 4.47$ %) compared to trials in which pulses had occurred prior to the response (i.e., response post-TMS: $M = 8.66$ %, $SD = 4.59$ %), irrespective of stimulation site. The main effect of stimulation site was only marginally significant ($\beta = –1.11$, $t(15.00) = –2.03$, $p = .061$). The interaction between stimulation site and TMS timing relative to response was not significant ($\beta = –0.79$, $t(15.00) = –0.80$, $p = .437$ $N = 16$, see Fig. 3B).

3.2. Response times

For response times, there was a significant main effect of trial type ($\beta = 25.66$, $t(14) = 10.05$, $p < .001$). Overall, responses were faster in error trials ($M = 239.40$ ms, $SD = 19.53$ ms) compared to correct trials ($M = 265.07$ ms, $SD = 18.41$ ms). The main effects of site and stimulation timing as well as the interaction between these factors were not significant (all *p*-values $\geq .119$, $n = 15$, see Fig. 3C).

3.3. EEG results

3.3.1. ERN based on the difference wave (ERN-diff)

Figure 4A provides response-locked grand-average ERP difference waves (error minus correct) at electrode FCz according to stimulation site (cerebellum, vertex) and stimulation timing (early, late), along with scalp topographies for the time points of maximum negativity in the ERN time window. Figure 4B displays corresponding response-locked grand-average ERPs for errors and correct responses.

There was a significant main effect of stimulation site ($\beta = 0.93$, $t(13.00) = 2.82$, $p = .015$). The ERN was less negative for cerebellar ($M = –5.56$ µV, $SD = 2.81$ µV) compared to vertex stimulation ($M = –6.49$ µV, $SD = 2.98$ µV). The main effect of timing was non-significant ($\beta = –0.02$, $t(13.00) = –0.05$, $p = .962$). The interaction of stimulation site and timing was significant ($\beta = –1.36$, $t(12.99) = –2.52$, $p = .026$). Simple slope analyses of the stimulation site for early and late stimulation timing yielded a significant slope (see Fig. S4 in the Supplementary Material) for late stimulation ($\beta = 1.61$, $t = 3.78$, $p < .001$). For early stimulation, the slope was non-significant ($\beta = 0.25$, $t = 0.59$, $p = .563$). The interaction between site and timing seemed to be driven by the late stimulation: for cerebellar TMS, the negativity was reduced for late ($M = –5.21$ µV, $SD = 2.72$ µV) compared to early stimulation ($M = –5.90$ µV,

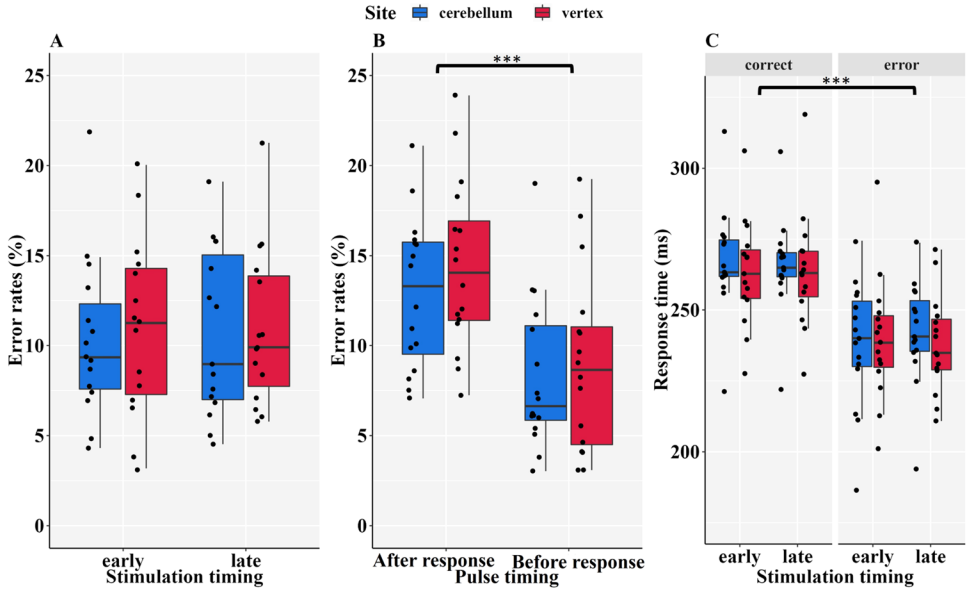

Fig. 3. (A) Mean error rates in Go trials according to stimulation site and stimulation timing. The analysis did not yield any significant effects of stimulation site or stimulation timing on error rates. (B) Mean error rates in Go trials according to stimulation site and pulse timing relative to response onset (i.e., whether a pulse had occurred prior to a response on a given trial or after the response). Asterisks indicate the significant main effect of pulse timing relative to response onset: error rates were higher in trials in which pulses had occurred after the response compared to trials in which pulses had occurred prior to response. (C) Mean response times in Go trials according to stimulation site and stimulation timing. Asterisks indicate the significant main effect of trial type: response times were shorter for errors compared to correct responses. The dots were jittered horizontally, the central line reflects the median and the whisker the first and third quartiles (the 25th and 75th percentiles) in all plots.

SD = 2.97 μV), and in contrast, vertex stimulation led to increased negativity for late (*M* = –6.82 μV, *SD* = 2.85 μV) compared to early stimulation (*M* = –6.16 μV, *SD* = 3.17 μV; see Fig. 5A for the boxplots of the ERN amplitudes as well as Fig. S4 for the interaction plot in the Supplementary Material).

3.3.2. *ERN in the original waveforms*

To elucidate whether the decreased negativity in the difference waves for cerebellar compared to vertex stimulation was specifically driven by altered neural responses to errors or correct responses, the original waveforms were analyzed (see Fig. 6). We found a significant main effect of trial type (β = 6.01, *t*(12.99) = 8.18, *p* > .001), with increased negativity for errors (*M* = –5.46 μV, *SD* = 3.98 μV) compared to correct responses (*M* = 0.55 μV, *SD* = 3.30 μV). All other main effects were non-significant (all $p \geq .079$). The interaction between trial type, and site was significant (β = –0.93, *t*(38.99) = –2.95, *p* = .005). Crucially, the three-way interaction between site, timing, and trial type was also significant (β = 1.36, *t*(38.99) = 2.16, *p* = .037). To resolve this interaction, we performed simple slope analysis. Results showed only a marginal significant slope for error trials on the stimulation sites and during late stimulation (β = 0.98, *t* = 2.06, *p* = .052). The slope was positive, indicating that the ERN was more negative in vertex (*M* = –5.78 μV, *SD* = 4.23 μV) compared to cerebellar stimulation (*M* = –5.13 μV, *SD* = 3.76 μV).

All other simple slopes for trial type, stimulation site, and stimulation timing were not significant (all $p \geq .200$).

3.3.3. *Pe-diff*

Analysis of the Pe in the difference waves did not yield any significant effects (all $p \geq .198$; see Fig. 5B for the boxplots of the Pe amplitudes).

4. DISCUSSION

This study investigated the role of the cerebellum in error processing using spTMS to stimulate the cerebellum while co-registering EEG. With the help of a Flanker pretask, we estimated individual ERN peak latencies and

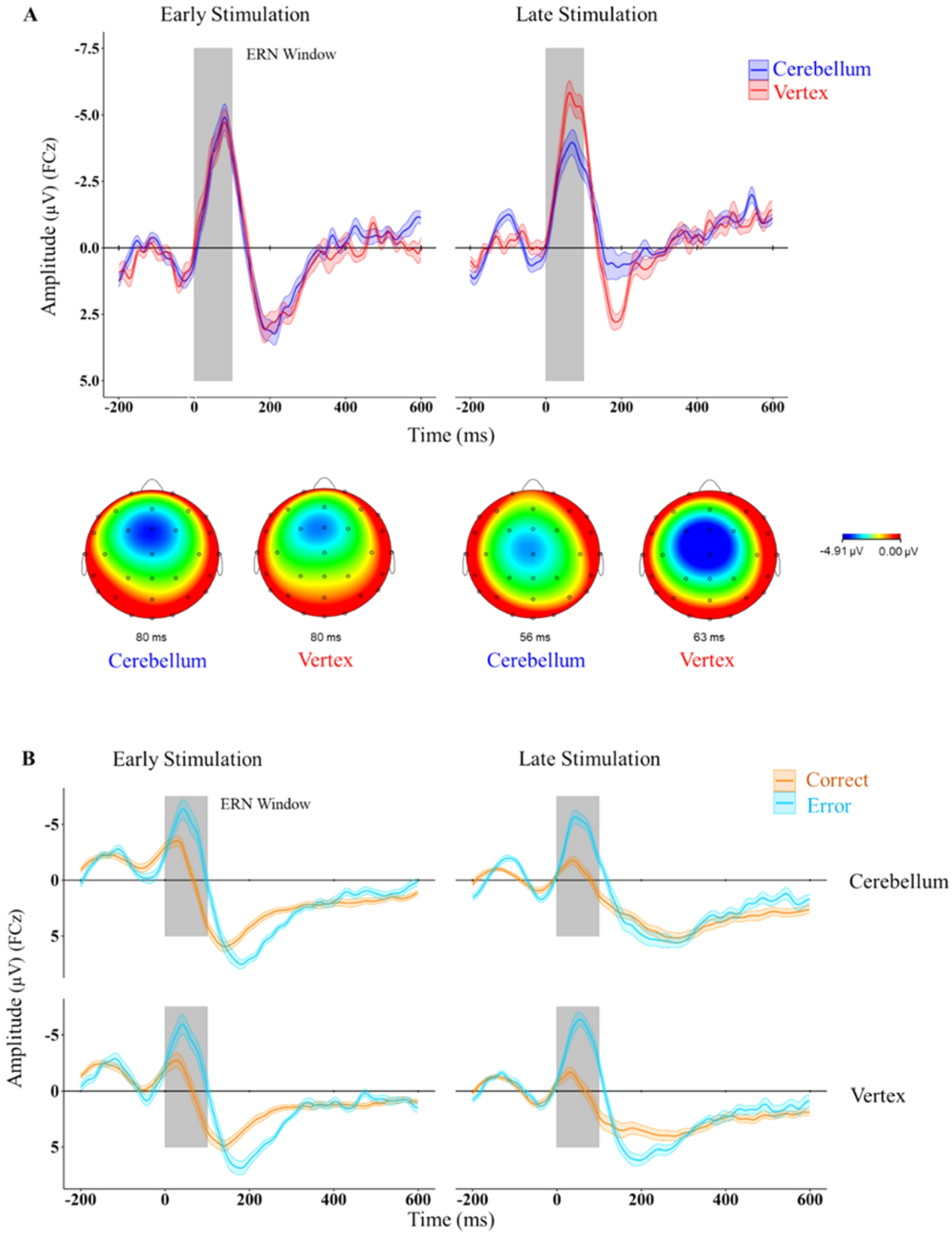

Fig. 4. (A) Response-locked grand-average ERP difference wave (error minus correct) at electrode FCz according to stimulation site (cerebellum, vertex) and stimulation timing (early, late), along with scalp topographies for the time points of maximum negativity in the ERN time window. (B) Response-locked grand-average ERPs for errors and correct responses at electrode FCz according to stimulation site (cerebellum, vertex) and stimulation timing (early, late) and trial type (correct, error). Smoothing around the lines in panel (A) and (B) indicate the standard error. The shaded area indicates time window for ERN quantification (0–100 ms post-response).

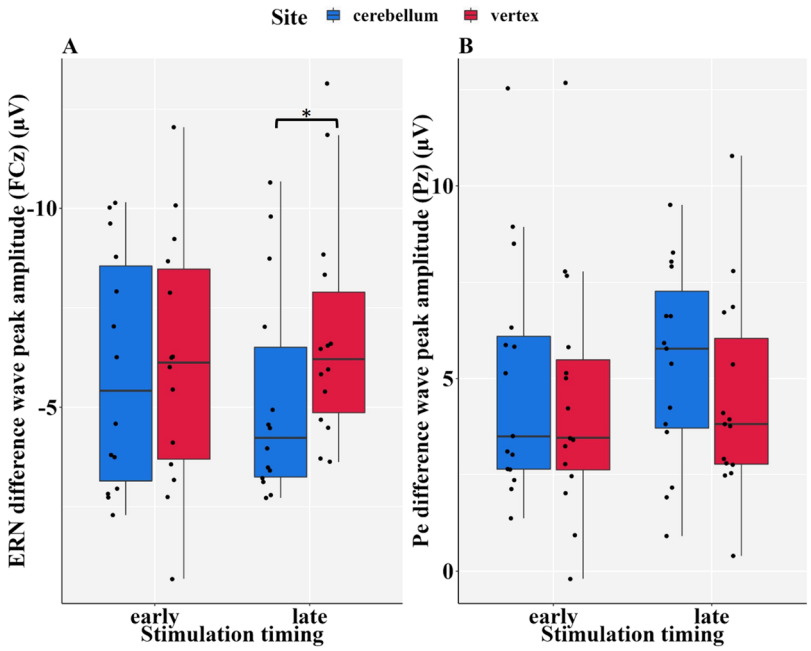

Fig. 5. (A) ERN peak amplitudes in the difference wave (error – correct) at electrode FCz as a function of stimulation site (cerebellum/vertex) and stimulation timing (early/late). Asterisks indicate the significant interaction effect between site and stimulation timing with the highly significant slope for late stimulation timing only. (B) Pe peak amplitudes in the difference wave (error – correct) at electrode Pz as a function of stimulation site (cerebellum/vertex) and stimulation timing (early/late). The dots were jittered horizontally. The central line reflects the median and the whisker the first and third quartiles (the 25th and 75th percentiles).

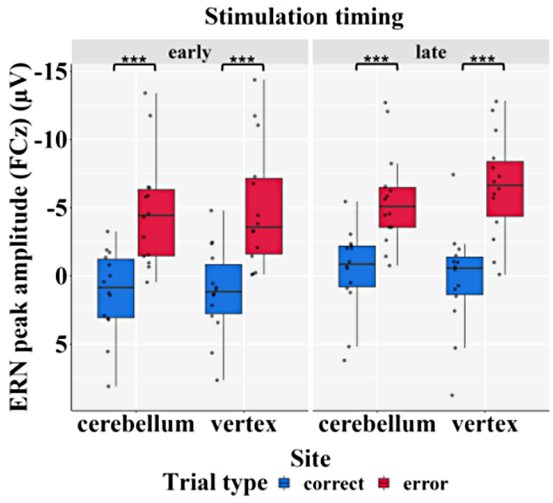

Fig. 6. ERN peak amplitudes as derived from the original waveforms at electrode FCz as a function of trial type (correct, error), stimulation site (cerebellum, vertex), and timing (early, late). Asterisks indicate significant main effects of trial type in both, cerebellar and vertex stimulation. All dots were jittered horizontally. The central line reflects the median and the whisker the first and third quartiles (the 25th and 75th percentiles).

median error response times to calculate the Individual Error Latency (IEL) as an approximation of the onset of error processing for each study participant. TMS pulses were then applied at different time points around the IEL in each trial of the subsequent Flanker main task. We expected to observe differences in error rates as well as in response-locked ERP components (specifically ERN, Pe) for cerebellar compared to vertex stimulation.

In line with our predictions, analysis of the ERP difference waves revealed that the ERN was reduced for cerebellar compared to vertex stimulation. This difference was also modulated by the timing of stimulation, with blunting particularly present for late compared to early stimulation. Analysis of the original ERP waveforms to determine whether the reduced negativity in the difference signal was particularly driven by altered neural responses to either errors or correct responses revealed that this effect was not specific to either response type.

Importantly, ERN magnitude in the Flanker pre-task was comparable between the day of cerebellar (M = –6.37 μV, SD = 2.09 μV) and vertex stimulation (M = –5.97 μV, SD = 2.18 μV, see Table S3 in the Supplementary Material). While we cannot exclude that active vertex stimulation

slightly increased the ERN (M = –6.49 μV, SD = 2.98 μV), ERN magnitude was substantially reduced for cerebellar stimulation (M = –5.56 μV, SD = 2.81 μV). Thus, the reduction of the ERN magnitude appeared to be driven mostly by spTMS applied to the cerebellum and not the vertex region, although vertex contributions cannot be fully excluded.

In general, the observed effect of stimulation site may indicate that monophasic single-pulse TMS disrupted inhibitory functions of the cerebellar cortex towards the deep cerebellar nuclei. This may have caused disinhibition, thereby facilitating information exchange with higher cortical structures through the cerebello-thalamo-cortical loop (Palesi et al., 2017). Here, the anterior cingulate cortex (ACC, Rubia et al., 2007), which is highly involved in the generation of the ERN (Dehaene et al., 1994; Holroyd & Coles, 2002), may be of particular interest. According to the reinforcement learning theory (Holroyd & Coles, 2002), the ERN is generated when a reduction of dopaminergic input from the VTA, possibly reflecting prediction errors, disinhibits deep cingulate cortical neurons. Recent findings show that the cerebellum may contribute to the generation of prediction errors. For instance, electrophysiological findings in mammals show that different cerebellar cell populations are sensitive to reward predictions and prediction violations (Heffley et al., 2018; Hull, 2020), and by the presence of direct cerebellar projections to the VTA that can modulate dopamine release in the striatum (Yoshida et al., 2022). Regarding the present results, with facilitated cerebello-cerebral information exchange, less phasic dopaminergic input towards the ACC may have reduced the cognitive demand for error processing (Holroyd & Coles, 2002).

In the conflict-monitoring theory (Botvinick et al., 2001, 2004), the ACC is seen as a monitoring system detecting conflicts (such as between opposing response options) and signaling the need for cognitive control. Here, facilitated cerebello-cerebral information exchange may have promoted conflict detection, leading to a reduced need for cognitive control that could be reflected in a reduced ERN. Adjustments in cognitive control related to conflict adaptation have previously been associated with increased functional interaction between prefrontal regions, superior temporal regions, and the anterior cerebellum (Egner & Hirsch, 2005). In addition, right cerebellar activation along with frontal and parietal activations were observed in the presence of persistent conflict leading to the interpretation that the cerebellum is involved in visuospatial attention processes during conflict to maintain high activation (Casey et al., 2000). However, somewhat contrary to both interpretations, error rates in the present study were not affected by cerebellar spTMS, and it could be argued that reduced cognitive demand or facilitated conflict detection should have led to increased accuracy/decreased error rates.

By taking advantage of the temporal resolution of spTMS, the present study addressed the question *when* cerebellar input is used during error processing. Our results show that late TMS pulses, that is, pulses that were applied to the cerebellum at IEL onset or shortly after, were more effective in that they were associated with a decrease in ERN magnitude in the error-correct difference signal. Early pulses, that is, pulses applied within 100 ms prior to IEL onset, left the ERN unaffected. A possible explanation for this pattern could be that the cerebellum receives information about the action through sensory input pathways and compares the actual information with the predicted outcome as stated in the forward model (Sokolov et al., 2017). Along these lines, cerebellar input for error processing is needed as this process is already underway. The peak of the ERN might correspond with the reconciliation of the predicted and actual action representation, that is., the use of the cerebellar input. Cerebellar spTMS may facilitate continuous information exchange with frontal regions by disinhibiting the cerebellar output signal. Thus, ERN generation would depend on this interplay of multiple regions, extending the existing framework (Falkenstein et al., 1991; Gehring et al., 1993) towards involvement of the cerebellum.

Analysis of the Pe in the difference signal did not reveal any significant effects of stimulation site or timing, which is in line with our hypothesis (see Fig. S5 of the grand averages in the Supplementary Material). The Pe likely reflects the conscious detection of an error (Endrass et al., 2007; Orr & Carrasco, 2011), and it is conceivable that error awareness might have been low due to the lack of feedback information in our rapid Go/Nogo Flanker task. Unfortunately, we did not implement any assessment of error awareness in the present study, so this notion remains speculative. Regardless of this, Pe alterations in the context of cerebellar damage were found in one previous study (Peterburs et al., 2012) in which patients with chronic cerebellar lesions were investigated. Here, an increase in Pe amplitudes—in concert with decreased ERN and preserved performance accuracy—was interpreted to reflect a compensatory mechanism. Importantly, spTMS to the cerebellum elicits a temporary effect while a stroke is associated with permanent tissue damage. Therefore, we can only roughly compare spTMS-induced "virtual lesions" of the cerebellum with degenerative or focal cerebellar diseases (Çan et al., 2018).

Analysis of the behavioral data showed no significant effects of site or timing. The lack of a site effect was unexpected, given that we had hypothesized an increase in error rates for cerebellar stimulation based on results observed in patients with cerebellar degeneration in an antisaccade task (Peterburs et al., 2015). However, another previous study also failed to find altered error rates in patients with cerebellar degeneration using a more comparable flanker task (Tunc et al., 2019). The present findings also resemble to some extent results obtained in patients with basal ganglia lesions, in whom the ERN was reduced in the absence of behavioral deficits in a flanker task (Ullsperger & von Cramon, 2006). In general, altered neural responses despite preserved behavior therefore are not particularly unusual. Interestingly, such a pattern of results has also been reported for feedback-based learning (Rustemeier et al., 2016) and in the acquisition phase of learning stimulus related contingencies in cerebellar lesion patients (Thoma et al., 2008), However, impaired learning performance in these patients was present when the task required reversal of learned stimulus-response-outcome contingencies (Thoma et al., 2008). Based on these observations, it could be speculated that the simple Flanker task used in the present study may not have been sensitive enough to detect more subtle performance differences as a function of stimulation site. It is conceivable that impaired cerebellar function may specifically affect behavioral flexibility, as suggested by findings of impaired feedback-based learning in cerebellar lesion patients only when the task involved reversal learning (Thoma et al., 2008). Behavioral flexibility is not tested in the Flanker task. Future studies could therefore investigate feedback-based learning and/or reversal learning in the context of cerebellar TMS.

When analyzing error rates according to TMS timing relative to response execution, we observed increased error rates in trials in which pulses had occurred after the response compared to trials in which pulses had occurred prior to response, irrespective of stimulation site. Thus, this effect is not informative about cerebellar contributions to error processing. Given that there were no baseline differences in error rates (based on flanker pre-task runs, see Fig. S1), this effect cannot be attributed to differences in baseline performance. It could, however, be speculated that the pulses themselves (regardless of where they were delivered) may have elicited a small startle response that could have slowed down subsequent responses. Along these lines, decreased error rates for trials in which pulses had occurred prior to the response could reflect a speed-accuracy trade-off, if increased accuracy after pre-response pulses coincided with increased response times. Unfortunately, response times could not be meaningfully analyzed according to TMS timing relative to response onset because stimulation timing was determined based on the IEL.

4.1. Limitations

This complex and technically advanced procedure led to some unique challenges and limitations that are relevant when interpreting the present results.

To begin, stimulation location was based on anatomical landmarks and not neuro-navigated. Moreover, the pulses were generated using two Magstim 200² in the Bistim configuration to overcome the challenge of the recharge period of the individual stimulators that is determined by the used output power, which varied greatly across the participants (see Table S1 in the Supplementary Material). Nevertheless, individual trials still had to be removed before analysis because no pulse had occurred. This was mostly due to the development of heat in the coil which caused the system to shut down so that the task was still running, and EEG was still recorded but no pulses were delivered. Here, the number of trials and breaks between the blocks need to be considered when planning a similarly fast-paced task in which monophasic single pulses are delivered across several hundreds of trials. Monophasic pulses are more likely to cause overheating due to the higher electrical charge compared to biphasic pulses (see Klomjai et al., 2015). Here, an external cooling system could help reduce heating issues.

Furthermore, the stimulation sites were the cerebellum and the vertex region, but we cannot exclude the possibility that stimulation also affected other brain regions. The direction of the magnetic field lines of the double cone coil are well-established to target deeper brain layers (Çan et al., 2018), but at the expense of a less focal stimulation in comparison to a figure-of-eight coil. Therefore, it may have caused stimulation of other, adjacent regions. This has been shown to be especially critical for vertex stimulation, which caused decreases in the BOLD signal in the default-mode network (see Jung et al., 2016). Regardless, we expected vertex stimulation to be a better control condition than sham because of a more comparable experience for participants regarding vibrations, coil click sounds, magnetic field build (Duecker & Sack, 2015), and discomfort. Some of the participants told us that they experienced the stimulation as uncomfortable, and that focusing on the task was

difficult because of the frequency of the pulses. Two participants dropped out in the cerebellar stimulation condition after the first block because they found the stimulation very unpleasant. The short trial period and jitter as well as the total number of trials might have contributed to this. Nevertheless, no systematic differences in ratings of these side effects were present between the two sessions, demonstrating that TMS pulses were perceived as similar for the stimulation sites (see Table S2 in the Supplementary Material).

In addition, Nogo trials and the analysis of response inhibition related ERP components were not the main focus of this work. This was partially due to the unexpectedly strong impact of TMS-induced EEG artifacts that hampered data analysis and result interpretation. In the grand-average ERPs for Nogo trials, the TMS induced artifacts did not completely disappear after preprocessing (see Fig. S7 in the Supplementary Material), and ERP components of interest, especially the Nogo-N2, occurred in close temporal proximity to pulses. We were able to identify the Nogo-N2 and Nogo-P3 to a certain degree, with grand-average patterns resembling those described in the literature (e.g., Rietdijk et al., 2014). The pulse artifact itself was cut out of the segment by the ARTIST algorithm, but there was still noise present that was likely caused by aftereffects (e.g., decay artifact) superimposed on the signal. Visual inspection of the grand-averages showed that the artifact was temporally shifted depending on pulse timing and more visible for vertex compared to cerebellar TMS, likely due to spatial proximity to analyzed electrode sites. Nevertheless, the grand-averages were also very similar to those obtained in the Go/Nogo pre-task without TMS pulses (see Fig. S2 for Go and Fig. S3 for Nogo ERPs in the Supplementary Material).

5. CONCLUSION

The present study investigated the role of the cerebellum for error processing using spTMS to stimulate the cerebellum while co-registering EEG. Applying cerebellar TMS caused a blunting of the ERN, directly supporting cerebellar involvement in performance monitoring. Of note, this effect was not specific to erroneous responses but generalized also to correct responses. Most importantly, our study also provides a first glimpse into temporal aspects of cerebellar contributions to error processing. The effect of cerebellar TMS on the ERN depended on pulse timing and was evident only when stimulation occurred around the onset of the IEL or shortly after. Finally, Pe as an index of late, more cognitive, awareness-related aspects of error processing, was not affected by cerebellar TMS.

In general, the present study adds to a growing body of research supporting cerebellar involvement in error processing and performance monitoring. More studies applying brain stimulation techniques are needed to further develop this line of research and investigate other aspects of performance monitoring such as feedback processing and feedback-based learning to better understand the role of the cerebellum for adaptive control of (non-motor) behavior.

DATA AND CODE AVAILABILITY

The data and code are openly available through the Open Science Framework at https://osf.io/jwfn9/

AUTHOR CONTRIBUTIONS

A.M.B., D.M.H., S.J.G., M.M., and J.P. planned the study. A.M.B. programmed the task. A.M.B. and D.M.H. set up the experiment, collected data, created the preprocessing pipeline, and analyzed the data. M.M. constructed the interface between the TMS and EEG system. J.P. supervised the project. A.M.B. and D.M.H. wrote the first draft of the manuscript. All authors contributed to results discussion and interpretation, and manuscript revision, and read and approved the submitted version.

FUNDING

This work was supported by the Deutsche Forschungsgemeinschaft (DFG) - Project number 437661157 awarded to J.P., M.M., and D.T.

DECLARATION OF COMPETING INTEREST

The study protocol was defined prior to the experiment and preregistered on osf.org (osf.io/6v9pa).

ACKNOWLEDGEMENT

We thank Greta Wippich for the illustration of the technical setup.

SUPPLEMENTARY MATERIAL

Supplementary material for this article is available with the online version here: https://doi.org/10.1162/imag_a_00080

REFERENCES

Bates, D., Mächler, M., Bolker, B., & Walker, S. (2014). Fitting linear mixed-effects models using lme4. *arXiv preprint* arXiv:1406.5823.

Botvinick, M. M., Braver, T. S., Barch, D. M., Carter, C. S., & Cohen, J. D. (2001). Conflict monitoring and cognitive control. *Psychological Review*, *108*(3), 624. https://psycnet.apa.org/doi/10.1037/0033-295X.108.3.624

Botvinick, M. M., Cohen, J. D., & Carter, C. S. (2004). Conflict monitoring and anterior cingulate cortex: An update. *Trends in Cognitive Sciences*, *8*(12), 539–546. https://doi.org/10.1016/j.tics.2004.10.003

Çan, M. K., Laakso, I., Nieminen, J. O., Murakami, T., & Ugawa, Y. (2018). Coil model comparison for cerebellar transcranial magnetic stimulation. *Biomedical Physics & Engineering Express*, *5*(1), 015020. https://doi.org/10.1088/2057-1976/aaee5b

Casey, B. J., Thomas, K. M., Welsh, T. F., Badgaiyan, R. D., Eccard, C. H., Jennings, J. R., & Crone, E. A. (2000). Dissociation of response conflict, attentional selection, and expectancy with functional magnetic resonance imaging. *Proceedings of the National Academy of Sciences*, *97*(15), 8728–8733. https://doi.org/10.1073/pnas.97.15.8728

Cavanagh, J. F., & Frank, M. J. (2014). Frontal theta as a mechanism for cognitive control. *Trends in Cognitive Sciences*, *18*(8), 414–421. https://doi.org/10.1016/j.tics.2014.04.012

Cohen, J. D., Botvinick, M., & Carter, C. S. (2000). Anterior cingulate and prefrontal cortex: Who's in control?. *Nature Neuroscience*, *3*(5), 421–423. https://doi.org/10.1038/74783

Cook, R. D. (1977). Detection of influential observation in linear regression. *Technometrics*, *19*(1), 15–18. https://doi.org/10.1080/00401706.1977.10489493

Danielmeier, C., Wessel, J. R., Steinhauser, M., & Ullsperger, M. (2009). Modulation of the error-related negativity by response conflict. *Psychophysiology*, *46*(6), 1288–1298. https://doi.org/10.1111/j.1469-8986.2009.00860.x

Dehaene, S., Posner, M. I., & Tucker, D. M. (1994). Localization of a neural system for error detection and compensation. *Psychological Science*, *5*(5), 303–305. https://doi.org/10.1111/j.1467-9280.1994.tb00630.x

Desmond, J. E., Chen, S. A., & Shieh, P. B. (2005). Cerebellar transcranial magnetic stimulation impairs verbal working memory. *Annals of Neurology*, *58*(4), 553–560. https://doi.org/10.1002/ana.20604

Duecker, F., & Sack, A. T. (2015). Rethinking the role of sham TMS. *Frontiers in Psychology*, *6*, 210. https://doi.org/10.3389/fpsyg.2015.00210

van Dun, K., Bodranghien, F., Manto, M., & Marien, P. (2017). Targeting the cerebellum by noninvasive neurostimulation: A review. *The Cerebellum*, *16*, 695–741. https://doi.org/10.1007/s12311-016-0840-7

Egner, T., & Hirsch, J. (2005). The neural correlates and functional integration of cognitive control in a Stroop task. *NeuroImage*, *24*(2), 539–547. https://doi.org/10.1016/j.neuroimage.2004.09.007

Endrass, T., Reuter, B., & Kathmann, N. (2007). ERP correlates of conscious error recognition: Aware and unaware errors in an antisaccade task. *European Journal of Neuroscience*, *26*(6), 1714–1720. https://doi.org/10.1111/j.1460-9568.2007.05785.x

Falkenstein, M., Hohnsbein, J., & Hoormann, J. (1995). Event-related potential correlates of errors in reaction tasks. *Electroencephalography and Clinical Neurophysiology*, *44*, 287–296. In G. Karmos, M. Molnar, V. Csepe, I. Czigler, & J. E. Desmedt (Eds.), *Perspectives of event-related potentials research* (EEG Journal Supplement 44) (pp. 280–286). Amsterdam: Elsevier.

Falkenstein, M., Hohnsbein, J., Hoormann, J., & Blanke, L. (1991). Effects of crossmodal divided attention on late ERP components. II. Error processing in choice reaction tasks. *Electroencephalography and Clinical Neurophysiology*, *78*, 447–455. https://doi.org/10.1016/0013-4694(91)90062-9

Ferdinand, N. K., Mecklinger, A., & Kray, J. (2008). Error and deviance processing in implicit and explicit sequence learning. *Journal of Cognitive Neuroscience*, *20*(4), 629–642. https://doi.org/10.1162/jocn.2008.20046

Fernandez, L., Major, B. P., Teo, W. P., Byrne, L. K., & Enticott, P. G. (2018). Assessing cerebellar brain inhibition (CBI) via transcranial magnetic stimulation (TMS): a systematic review. *Neuroscience & Biobehavioral Reviews*, *86*, 176–206. https://doi.org/10.1016/j.neubiorev.2017.11.018

Folstein, J. R., & Van Petten, C. (2008). Influence of cognitive control and mismatch on the N2 component of the ERP: A review. *Psychophysiology*, *45*(1), 152–170. https://doi.org/10.1111/j.1469-8986.2007.00602.x

Gehring, W. J., Goss, B., Coles, M. G., Meyer, D. E., & Donchin, E. (1993). A neural system for error detection and compensation. *Psychological Science*, *4*, 385–390. https://doi.org/10.1111/j.1467-9280.1993.tb00586.x

Grimaldi, G., Argyropoulos, G. P., Boehringer, A., Celnik, P., Edwards, M. J., Ferrucci, R., Galea, J. M., Groiss, S. J., Hiraoka, K., Kassavetis, P., Lesage, E., Manto, M., Miall, R. C., Priori, A., Sadnicka, A., Ugawa, Y., & Ziemann, U. (2014). Non-invasive cerebellar stimulation—A consensus paper. *The Cerebellum*, *13*, 121–138. https://doi.org/10.1007/s12311-013-0514-7

Hajcak, G., & Foti, D. (2008). Errors are aversive: Defensive motivation and the error-related negativity. *Psychological Science*, *19*(2), 103–108. https://doi.org/10.1111/j.1467-9280.2008.02053.x

Hardwick, R. M., Lesage, E., & Miall, R. C. (2014). Cerebellar transcranial magnetic stimulation: The role of coil geometry and tissue depth. *Brain Stimulation*, *7*(5), 643–649. https://doi.org/10.1016/j.brs.2014.04.009

Heffley, W., Song, E. Y., Xu, Z., Taylor, B. N., Hughes, M. A., McKinney, A., Joshua, M., & Hull, C. (2018). Coordinated cerebellar climbing fiber activity signals learned sensorimotor predictions. *Nature Neuroscience*, *21*(10), 1431–1441. https://doi.org/10.1038/s41593-018-0228-8

Hernandez-Pavon, J. C., Veniero, D., Bergmann, T. O., Belardinelli, P., Bortoletto, M., Casarotto, S., Casula, E. P., Farzan, F., Fecchio, M., Julkunen, P., Kallioniemi, E., Lioumis, P., Metsomaa, J., Miniussi, C., Mutanen, T. P., Rocchi, L., Rogasch, N. C., Shafi, M. M., Siebner, H. R., … Ilmoniemi, R. J. (2023). TMS combined with EEG: Recommendations and open issues for data collection and analysis. *Brain Stimulation*, *16*(2), 567–593. https://doi.org/10.1016/j.brs.2023.02.009

Herrmann, M. J., Römmler, J., Ehlis, A. C., Heidrich, A., & Fallgatter, A. J. (2004). Source localization (LORETA) of the error-related-negativity (ERN/Ne) and positivity (Pe). *Cognitive Brain Research*, *20*(2), 294–299. https://doi.org/10.1016/j.cogbrainres.2004.02.013

Holroyd, C. B., & Coles, M. G. (2002). The neural basis of human error processing: Reinforcement learning,

dopamine, and the error-related negativity. *Psychological Review*, *109*(4), 679. https://doi.org/10.1037/0033-295X.109.4.679

Holroyd, C. B., & Yeung, N. (2011). An integrative theory of anterior cingulate cortex function: Option selection in hierarchical reinforcement learning. *Neural Basis of Motivational and Cognitive Control*, *16*, 333–349. https://doi.org/10.7551/mitpress/9780262016438.003.0018

Hull, C. (2020). Prediction signals in the cerebellum: Beyond supervised motor learning. *elife*, *9*, e54073. https://doi.org/10.7554/eLife.54073

Ito, M. (2008). Control of mental activities by internal models in the cerebellum. *Nature Reviews Neuroscience*, *9*(4), 304–313. https://doi.org/10.1038/nrn2332

Jalali, R., Miall, R. C., & Galea, J. M. (2017). No consistent effect of cerebellar transcranial direct current stimulation on visuomotor adaptation. *Journal of Neurophysiology*, *118*(2), 655–665. https://doi.org/10.1152/jn.00896.2016

Jung, J., Bungert, A., Bowtell, R., & Jackson, S. R. (2016). Vertex stimulation as a control site for transcranial magnetic stimulation: A concurrent TMS/fMRI study. *Brain Stimulation*, *9*(1), 58–64. https://doi.org/10.1016/j.brs.2015.09.008

King, M., Hernandez-Castillo, C. R., Poldrack, R. A., Ivry, R. B., & Diedrichsen, J. (2019). Functional boundaries in the human cerebellum revealed by a multi-domain task battery. *Nature Neuroscience*, *22*(8), 1371–1378. https://doi.org/10.1038/s41593-019-0436-x

Klein, P. A., Petitjean, C., Olivier, E., & Duque, J. (2014). Top-down suppression of incompatible motor activations during response selection under conflict. *NeuroImage*, *86*, 138–149. https://doi.org/10.1016/j.neuroimage.2013.08.005

Klomjai, W., Katz, R., & Lackmy-Vallée, A. (2015). Basic principles of transcranial magnetic stimulation (TMS) and repetitive TMS (rTMS). *Annals of Physical and Rehabilitation Medicine*, *58*(4), 208–213. https://doi.org/10.1016/j.rehab.2015.05.005

Koponen, L. M., Nieminen, J. O., Mutanen, T. P., & Ilmoniemi, R. J. (2018). Noninvasive extraction of microsecond-scale dynamics from human motor cortex. *Human Brain Mapping*, *39*(6), 2405–2411. https://doi.org/10.1002/hbm.24010

Koziol, L. F., Budding, D., Andreasen, N., D'Arrigo, S., Bulgheroni, S., Imamizu, H., Ito, M., Manto, M., Marvel, C., Parker, K., Pezzulo, G., Ramnani, N., Riva, D., Schmahmann, J., Vandervert, L., & Yamazaki, T. (2014). Consensus paper: The cerebellum's role in movement and cognition. *The Cerebellum*, *13*, 151–177. https://doi.org/10.1007/s12311-013-0511-x

Kuznetsova, A., Brockhoff, P. B., & Christensen, R. H. (2017). lmerTest package: Tests in linear mixed effects models. *Journal of Statistical Software*, *82*, 1–26. https://doi.org/10.18637/jss.v082.i13

Larson, M. J., Baldwin, S. A., Good, D. A., & Fair, J. E. (2010). Temporal stability of the error-related negativity (ERN) and post-error positivity (Pe): The role of number of trials. *Psychophysiology*, *47*(6), 1167–1171. https://doi.org/10.1111/j.1469-8986.2010.01022.x

Larson, M. J., & Clayson, P. E. (2011). The relationship between cognitive performance and electrophysiological indices of performance monitoring. *Cognitive, Affective, & Behavioral Neuroscience*, *11*, 159–171. https://doi.org/10.3758/s13415-010-0018-6

Lehrl, S., Merz, J., & Burkhard, G. F. S. (1977). *Mehrfachwahl-Wortschatz-Test (MWT-B)*. Erlangen: Straube.

Mannarelli, D., Pauletti, C., Petritis, A., Delle Chiaie, R., Currà, A., Trompetto, C., & Fattapposta, F. (2020). Effects of cerebellar tDCS on inhibitory control: Evidence from a Go/NoGo task. *The Cerebellum*, *19*, 788–798. https://doi.org/10.1007/s12311-020-01165-z

Meteyard, L., & Davies, R. A. (2020). Best practice guidance for linear mixed-effects models in psychological science. *Journal of Memory and Language*, *112*, 104092. https://doi.org/10.1016/j.jml.2020.104092

Nieuwenhuis, R., te Grotenhuis, M., & Pelzer, B. (2012). Influence.ME: Tools for detecting influential data in mixed effects models. *R Journal*, *4*(2), 38–47. https://doi.org/10.32614/rj-2012-011

Olvet, D. M., & Hajcak, G. (2009). The stability of error-related brain activity with increasing trials. *Psychophysiology*, *46*(5), 957–961. https://doi.org/10.1111/j.1469-8986.2009.00848.x

Orr, J. M., & Carrasco, M. (2011). The role of the error positivity in the conscious perception of errors. *Journal of Neuroscience*, *31*(16), 5891–5892. https://doi.org/10.1523/JNEUROSCI.0279-11.2011

Palesi, F., Rinaldis, A. de, Castellazzi, G., Calamante, F., Muhlert, N., Chard, D., Tournier, J. D., Magenes, G., D'Angelo, E., & Gandini Wheeler-Kingshott, C. A. M. (2017). Contralateral cortico-ponto-cerebellar pathways reconstruction in humans in vivo: Implications for reciprocal cerebro-cerebellar structural connectivity in motor and non-motor areas. *Scientific Reports*, *7*(1), 12841. https://doi.org/10.1038/s41598-017-13079-8

Panouillères, M., Neggers, S. F., Gutteling, T. P., Salemme, R., Stigchel, S. V. D., van der Geest, J. N., … & Pelisson, D. (2012). Transcranial magnetic stimulation and motor plasticity in human lateral cerebellum: Dual effect on saccadic adaptation. *Human Brain Mapping*, *33*(7), 1512–1525. https://doi.org/10.1002/hbm.21301

Pascual-Leone, A. (1999). Transcranial magnetic stimulation: Studying the brain–behaviour relationship by induction of 'virtual lesions'. *Philosophical Transactions of the Royal Society of London. Series B: Biological Sciences*, *354*(1387), 1229–1238. https://doi.org/10.1098/rstb.1999.0476

Peterburs, J., & Desmond, J. E. (2016). The role of the human cerebellum in performance monitoring. *Current Opinion in Neurobiology*, *40*, 38–44. https://doi.org/10.1016/j.conb.2016.06.011

Peterburs, J., Gajda, K., Koch, B., Schwarz, M., Hoffmann, K. P., Daum, I., & Bellebaum, C. (2012). Cerebellar lesions alter performance monitoring on the antisaccade task—An event-related potentials study. *Neuropsychologia*, *50*(3), 379–389. https://doi.org/10.1016/j.neuropsychologia.2011.12.009

Peterburs, J., Thürling, M., Rustemeier, M., Göricke, S., Suchan, B., Timmann, D., & Bellebaum, C. (2015). A cerebellar role in performance monitoring–Evidence from EEG and voxel-based morphometry in patients with cerebellar degenerative disease. *Neuropsychologia*, *68*, 139–147. https://doi.org/10.1016/j.neuropsychologia.2015.01.017

Pizem, D., Novakova, L., Gajdos, M., & Rektorova, I. (2022). Is the vertex a good control stimulation site? Theta burst stimulation in healthy controls. *Journal of Neural Transmission*, *129*(3), 319–329. https://doi.org/10.1007/s00702-022-02466-9

Pontifex, M. B., Scudder, M. R., Brown, M. L., O'Leary, K. C., Wu, C. T., Themanson, J. R., & Hillman, C. H.

(2010). On the number of trials necessary for stabilization of error-related brain activity across the life span. *Psychophysiology*, *47*(4), 767–773. https://doi.org/10.1111/j.1469-8986.2010.00974.x

Ramnani, N. (2006). The primate cortico-cerebellar system: Anatomy and function. *Nature Reviews Neuroscience*, *7*(7), 511–522. https://doi.org/10.1038/nrn1953

Rietdijk, W. J., Franken, I. H., & Thurik, A. R. (2014). Internal consistency of event-related potentials associated with cognitive control: N2/P3 and ERN/Pe. *PloS One*, *9*(7), e102672. https://doi.org/10.1371/journal.pone.0102672

Rogasch, N. C., Sullivan, C., Thomson, R. H., Rose, N. S., Bailey, N. W., Fitzgerald, P. B., Farzan, F., & Hernandez-Pavon, J. C. (2017). Analysing concurrent transcranial magnetic stimulation and electroencephalographic data: A review and introduction to the open-source TESA software. *NeuroImage*, *147*, 934–951. https://doi.org/10.1016/j.neuroimage.2016.10.031

RStudio Team. (2020). *RStudio: Integrated Development for R*. Boston, MA: RStudio, PBC, http://www.rstudio.com/

Rubia, K., Smith, A. B., Taylor, E., & Brammer, M. (2007). Linear age-correlated functional development of right inferior fronto-striato-cerebellar networks during response inhibition and anterior cingulate during error-related processes. *Human Brain Mapping*, *28*(11), 1163–1177. https://doi.org/10.1002/hbm.20347

Rustemeier, M., Koch, B., Schwarz, M., & Bellebaum, C. (2016). Processing of positive and negative feedback in patients with cerebellar lesions. *The Cerebellum*, *15*(4), 425–438. https://doi.org/10.1007/s12311-015-0702-8

Sheu, Y. S., Liang, Y., & Desmond, J. E. (2019). Disruption of cerebellar prediction in verbal working memory. *Frontiers in Human Neuroscience*, *13*, 61. https://doi.org/10.3389/fnhum.2019.00061

Shirota, Y., Hamada, M., Terao, Y., Ohminami, S., Tsutsumi, R., Ugawa, Y., & Hanajima, R. (2012). Increased primary motor cortical excitability by a single-pulse transcranial magnetic stimulation over the supplementary motor area. *Experimental Brain Research*, *219*, 339–349. https://doi.org/10.1007/s00221-012-3095-7

Sokolov, A. A., Miall, R. C., & Ivry, R. B. (2017). The cerebellum: Adaptive prediction for movement and cognition. *Trends in Cognitive Sciences*, *21*(5), 313–332. https://doi.org/10.1016/j.tics.2017.02.005

Soto, D., Montoro, P. R., & Humphreys, G. W. (2009). Transcranial magnetic stimulation of the primary motor cortex modulates response interference in a flanker task. *Neuroscience Letters*, *451*(3), 261–265. https://doi.org/10.1016/j.neulet.2008.12.052

Stoodley, C. J., & Schmahmann, J. D. (2009). Functional topography in the human cerebellum: A meta-analysis of neuroimaging studies. *NeuroImage*, *44*(2), 489–501. https://doi.org/10.1016/j.neuroimage.2008.08.039

Thoma, P., Bellebaum, C., Koch, B., Schwarz, M., & Daum, I. (2008). The cerebellum is involved in reward-based reversal learning. *The Cerebellum*, *7*, 433–443. https://doi.org/10.1007/s12311-008-0046-8

Tunc, S., Baginski, N., Lubs, J., Bally, J. F., Weissbach, A., Baaske, M. K., Tadic, V., Brüggemann, N., Bäumer, T., Beste, C., & Münchau, A. (2019). Predictive coding and adaptive behavior in patients with genetically determined cerebellar ataxia—A neurophysiology study. *NeuroImage: Clinical*, *24*, 102043. https://doi.org/10.1016/j.nicl.2019.102043

Ugawa, Y., Uesaka, Y., Terao, Y., Hanajima, R., & Kanazawa, I. (1995). Magnetic stimulation over the cerebellum in humans. *Annals of Neurology*, *37*(6), 703–713. https://doi.org/10.1002/ana.410370603

Ullsperger, M., & von Cramon, D. Y. (2006). The role of intact frontostriatal circuits in error processing. *Journal of Cognitive Neuroscience*, *18*(4), 651–664. https://doi.org/10.1162/jocn.2006.18.4.651

Vaidya, A. R., Pujara, M. S., Petrides, M., Murray, E. A., & Fellows, L. K. (2019). Lesion studies in contemporary neuroscience. *Trends in Cognitive Sciences*, *23*(8), 653–671. https://doi.org/10.1016/j.tics.2019.05.009

Van Veen, V., & Carter, C. S. (2002). The anterior cingulate as a conflict monitor: fMRI and ERP studies. *Physiology & Behavior*, *77*(4–5), 477–482. https://doi.org/10.1016/S0031-9384(02)00930-7

Verleger, R., Kuniecki, M., Möller, F., Fritzmannova, M., & Siebner, H. R. (2009). On how the motor cortices resolve an inter-hemispheric response conflict: An event-related EEG potential-guided TMS study of the flankers task. *European Journal of Neuroscience*, *30*(2), 318–326. https://doi.org/10.1111/j.1460-9568.2009.06817.x

Voegler, R., Peterburs, J., Lemke, H., Ocklenburg, S., Liepelt, R., & Straube, T. (2018). Electrophysiological correlates of performance monitoring under social observation in patients with social anxiety disorder and healthy controls. *Biological Psychology*, *132*, 71–80. https://doi.org/10.1016/j.biopsycho.2017.11.003

Wolpert, D. M., Miall, R. C., & Kawato, M. (1998). Internal models in the cerebellum. *Trends in cognitive Sciences*, *2*(9), 338–347. https://doi.org/10.1016/S1364-6613(98)01221-2

Wu, W., Keller, C. J., Rogasch, N. C., Longwell, P., Shpigel, E., Rolle, C. E., & Etkin, A. (2018). ARTIST: A fully automated artifact rejection algorithm for single-pulse TMS-EEG data. *Human Brain Mapping*, *39*(4), 1607–1625. https://doi.org/10.1002/hbm.23938

Yeung, N., Botvinick, M. M., & Cohen, J. D. (2004). The neural basis of error detection: Conflict monitoring and the error-related negativity. *Psychological Review*, *111*(4), 931–959. https://doi.org/10.1037/0033-295X.111.4.931

Yoshida, J., Oñate, M., Khatami, L., Vera, J., Nadim, F., & Khodakhah, K. (2022). Cerebellar contributions to the basal ganglia influence motor coordination, reward processing, and movement vigor. *Journal of Neuroscience*, *42*(45), 8406–8415. https://doi.org/10.1523/JNEUROSCI.1535-22.2022